J Math Chem (2012) 50:2512–2526
DOI 10.1007/s10910-012-0046-2

ORIGINAL PAPER

Interaction of double-stranded DNA inside single-walled carbon nanotubes

Mansoor H. Alshehri · Barry J. Cox · James M. Hill

Received: 4 April 2012 / Accepted: 11 June 2012 / Published online: 22 June 2012

Abstract Deoxyribonucleic acid (DNA) is the genetic material for all living organisms, and as a nanostructure offers the means to create novel nanoscale devices. In this paper, we investigate the interaction of deoxyribonucleic acid inside single-walled carbon nanotubes. Using classical applied mathematical modeling, we derive explicit analytical expressions for the encapsulation of DNA inside single-walled carbon nanotubes. We adopt the 6–12 Lennard–Jones potential function together with the continuous approach to determine the preferred minimum energy position of the dsDNA molecule inside a single-walled carbon nanotube, so as to predict its location with reference to the cross-section of the carbon nanotube. An analytical expression is obtained in terms of hypergeometric functions which provides a computationally rapid procedure to determine critical numerical values. We observe that the double-strand DNA can be encapsulated inside a single-walled carbon nanotube with a radius larger than 12.30 Å, and we show that the optimal single-walled carbon nanotube to enclose a double-stranded DNA has radius 12.8 Å.

Keywords Deoxyribonucleic acid (DNA) · Single-walled carbon nanotube (SWCNT) · Lennard-Jones potential · Continuous approach

1 Introduction

Classical applied mathematics and mechanics generate models to predict ideal behavior and to determine simple but relevant solutions which provide insight into complex physical processes. In many disciplines, applied mathematical modelling has been

M. H. Alshehri (✉) · B. J. Cox · J. M. Hill
The University of Adelaide, Adelaide, SA, Australia
e-mail: mansoor.alshehri@adelaide.edu.au

used to determine elegant solutions to problems, but thus far, few problems have been addressed in nanotechnology. Recently, the characterization of nano-materials and the design and realization of nanostructure based devices with advanced functionality has had an impact on the field of materials science and micro-engineering [6]. Since the discovery of the double helix structure of deoxyribonucleic acid (DNA) by Watson and Crick in 1953 [24], DNA has also generated much research interest, and recently several areas in modern biotechnology have shown considerable potential for DNA molecules in the construction of nanostructures and devices, such as the assembly of devices and computational elements, for the assembly of interconnects, or as the device element itself [19]. In addition, the encapsulation of biomolecules such as DNA has promised many applications in gene and drug delivery [12]. Furthermore, inorganic nanomaterials involving carbon nanotubes (CNTs), nanocrystals, and nanowires with their unique physical and chemical properties have generated attention for future applications such as drug delivery, enzyme immobilization, and DNA transfection [15,16,19]. The functionalization of CNTs with DNA has recently aroused interest in the developing area of nanobiotechnology due to many potential applications in molecular electronics, field devices and medical applications [3,8,21]. These applications of DNA with CNTs have increased the interest in CNT solubility in organic media and DNA assisted CNT characterisation [1,22,27,28].

Xu et al. [25] use a tight-binding method combined with molecular dynamics (MD) simulations to investigete the electrostatic signals generated by DNA segments inside short semiconducting single-walled carbon nanotubes, and they obtain stronger electrical signals for the semiconducting CNTs when DNA bases are present inside the CNT. Shim et al. [22] focus on encapsulating DNA molecules inside CNTs, while Cui et al. [5] show that the double stranded DNA molecules can be encapsulated inside multiwalled carbon nanotubes in water at 400 K and 3 Bar. In addition, by employing the (MD) simulation to study the translocating of dsDNA molecules through single wall carbon nanotube, Xue and Chen [26] show that the dsDNA molecules could be inserted into (20, 20) CNT within 100 ps in vacuo. Lau et al. [17] investigate the encapsulation of double-stranded DNA inside single-walled carbon nanotubes of diameters 30 and 40 Å, using (MD) simulation. They find that the structure of dsDNA is not significantly perturbed if the counterions are included inside the nanotube. Ito et al. [14] study the transport of the dsDNA molecule through a multiwalled carbon nanotube with 77 nm in diameter by fluorescence microscopy.

In the present work, we study the equilibrium position for a double helix DNA molecule inside a single-wall carbon nanotube (SWCNT), and by minimizing the interaction energy between the DNA and the CNT, we deduce the optimal radius of the CNT which can be used to accommodate the DNA. In particular, we assume the B-DNA form which is the structure commonly found inside cells [2,21]. With reference to Fig. 1, we consider a unit cell comprising a DNA molecule over a distance of 34 Å. The DNA groove sites refer to the spaces between the strands, and there are two groove sites which are created by the coiling of the two helices around each other; the wider one is called the major groove which is 22 Å in length, and the smaller is called the minor groove which in is 12 Å in length [2]. We join the two helices with a continuum of straight, horizontal lines forming a surface which resembles that of a twisted ribbon and which we use to model the structure of the DNA unit cell.

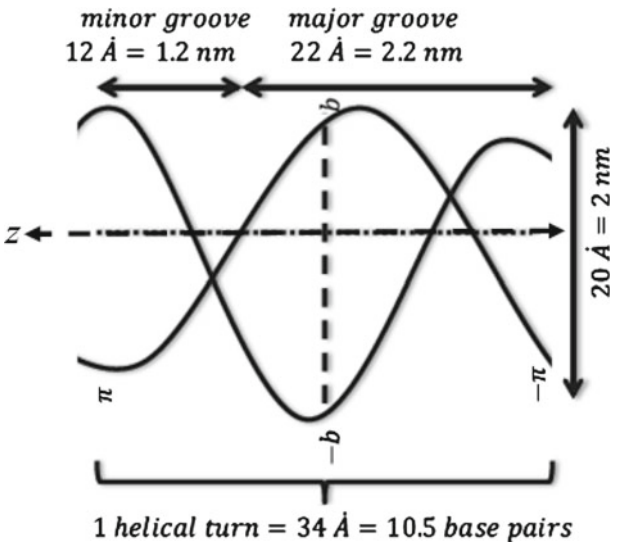

Fig. 1 Assumed geometry of double helix B-DNA for one turn of helix (34 Å)

The DNA comprises five elements: carbon (C), oxygen (O), hydrogen (H), nitrogen (N) and phosphorus (P) [2,11,18,23]. There are approximately 21 nucleotides that make up one turn of the dsDNA; each nucleotide is composed of deoxyribose sugar attached to a single phosphate group and the base which may be either guanine (G), cytosine (C), adenine (A) and thymine (T). After taking the average of atoms of 21 bases and adding them to the atoms of the deoxyribose sugar and the phosphate group, we have 204.75 carbon atoms, 189 oxygen atoms, 299.25 hydrogen atoms, 78.75 nitrogen atoms and 21 phosphorus atoms, which gives a total average of 792.75 atoms in the unit cell. The modeling proposed here is not intended to compute all the detail of the underlying physics, but rather to represent the most important interactions for the purpose of determining the dominant phenomena of the system. In addition, the theoretical results presented in this paper might pave the way toward further developing the area.

In Sect. 2, we introduce the Lennard-Jones potential and the continuous approach which assumes an average atomic surface density of the atoms on the DNA molecule and an average surface density of carbon atoms on the nanotube. We comment that Girifalco et al. [9] state that the continuum Lennard-Jones approach may in many instances be a good approximation for uniform atomic distributions. In Sect. 3.1, we present the details for the derivation of the total interaction energy per unit length for the DNA molecule which is assumed to be located inside the single-walled carbon nanotube. In addition, in Sect. 3.2, we also give the corresponding calculation for the special case of the interaction between the atoms of DNA and the carbon nanotube surface when the helical phase angle $\phi = \pi$, and some conclusions are presented in Sect. 4. In Appendices A and B we present the analytical details for the interaction energy for any value of the helical phase angle ϕ and for the specific value $\phi = \pi$, respectively.

2 Atomic interaction potentials

2.1 Lennard-Jones potential

The total non-bonded interaction energy E, may be obtained by summing the interaction energy for each atomic pair and is given by

$$E = \sum_i \sum_j P(\rho_{ij}),$$

where $P(\rho_{ij})$ is a potential function for atoms i and j which are separated by a distance ρ_{ij}. In the continuous approximation, the atoms are assumed to be uniformly distributed over the surface of the molecules, and so we replace the double summation by two surface integrals, thus

$$E = \eta_1 \eta_2 \int_{S_1} \int_{S_2} P(\rho)\, dS_1\, dS_2,$$

where η_1 and η_2 are atomic surface densities of the first and the second molecules, respectively, and ρ is the distance between two typical surface elements dS_1 and dS_2 on the two unbonded molecules. In this paper, we adopt the 6–12 Lennard–Jones potential to determine the van der Waals interaction energy. The classical Lennard-Jones potential for two atoms at a distance ρ apart is given by

$$P(\rho) = 4\varepsilon\Big[-\Big(\frac{\sigma}{\rho}\Big)^6 + \Big(\frac{\sigma}{\rho}\Big)^{12}\Big],$$

where ρ is the distance between two atoms, ε is the magnitude of the energy at the equilibrium distance $\rho_0 = 2^{1/6}\sigma$, and σ is the atomic distance when the potential energy is zero. The constants ε and σ are determined experimentally and if given the values ε_1, σ_1 for the interaction of the atoms of one species and ε_2, σ_2 for the interaction of the atoms of a second species, then these parameters for the interaction of atoms of species 1 with those of species 2 may be determined from the empirical mixing rules given by $\varepsilon_{12} = (\varepsilon_1 \varepsilon_2)^{1/2}$, and $\sigma_{12} = (\sigma_1 + \sigma_2)/2$ [9,13]. The 6–12 Lennard–Jones potential may also be expressed as

$$P(\rho) = -\frac{A}{\rho^6} + \frac{B}{\rho^{12}},$$

where A and B are called the attractive and the repulsive constants, respectively, and are given in terms of the previously given parameters given previously by $A = 4\varepsilon\sigma^6$ and $B = 4\varepsilon\sigma^{12}$. Table 1 gives numerical values of the Lennard-Jones constants for the particular elements studied in this paper. To determine the total interaction energy for two non-bonded molecules we use the Lennard-Jones potential function for two non-bonded molecules with the continuous approximation which is given by

Table 1 Lennard-Jones force constants [20]

	$\varepsilon(\text{eV} \times 10^{-2})$	σ (Å)
C–C	0.4119	3.88
C–H	0.1336	3.54
C–N	0.5089	3.7875
C–O	0.6197	3.695
C–P	0.6197	4.0875

$$E = \eta_1 \eta_2 \int_{S_1} \int_{S_2} \left(-\frac{A}{\rho^6} + \frac{B}{\rho^{12}} \right) dS_1\, dS_2,$$

where η_1 and η_2 are atomic surface densities of the first and the second molecules, respectively.

2.2 DNA and CNT geometry

In this study, we model the DNA as a surface with the double helical geometry located on the z-axis, as shown in Fig. 1. With reference to a rectangular Cartesian coordinate system (x, y, z), a typical point on the surface of the DNA is given by

$$\mathbf{R}(\theta_1, t) = \left(\frac{r}{2}\Big[\cos\theta_1 + \cos(\theta_1 - \phi) + t\Big(\cos\theta_1 - \cos(\theta_1 - \phi)\Big)\Big], \right.$$
$$\left. \frac{r}{2}\Big[\sin\theta_1 + \sin(\theta_1 - \phi) + t\Big(\sin\theta_1 - \sin(\theta_1 - \phi)\Big)\Big], \frac{c\theta_1}{2\pi} \right),$$

where $r = 10$ Å is the radius of the DNA helix, $c = 34$ Å is the unit cell length, $\phi = 12\pi/17$ is the helical phase angle parameter and the parametric variable t is such that $-1 < t < 1$, and $-\pi < \theta_1 < \pi$. Similarly, with reference to the rectangular Cartesian coordinate system (x, y, z) with origin located at the centre of the nanotube, a typical point on the surface of the tube has the coordinates $(a\cos\theta_2, a\sin\theta_2, z)$, where a is the radius of the carbon nanotube and $-\infty < z < \infty$ and $-\pi < \theta_2 < \pi$. Thus, the distance ρ between a typical surface element on the CNT and another on the DNA is given by

$$\rho^2 = a^2 - ar\big[\cos(\theta_1-\theta_2) + \cos(\theta_1-\theta_2-\phi) + t[\cos(\theta_1-\theta_2) - \cos(\theta_1-\theta_2-\phi)]\big]$$
$$+ r^2\Big[\cos^2(\phi/2) + t^2\sin^2(\phi/2)\Big] + (z - c\theta_1/2\pi)^2.$$

3 Interaction of carbon nanotube with DNA

3.1 General case

In this section, we consider the general helical angle ϕ for which we have in mind the particular value $\phi = 12\pi/17$ which leads to the major and minor groove sites mentioned above. The equilibrium position is the location of the minimum potential energy for the DNA inside the CNT. We begin by considering the interaction of a carbon nanotube with a single point situated at a distance ξ from the tube axis, as shown in Fig. 2. We then integrate this potential for a single point over the surface of the DNA molecule, thus (Table 2)

$$\begin{aligned}\xi^2 &= \left(\frac{r}{2}[\cos\theta_1 + \cos(\theta_1 - \phi) + t(\cos\theta_1 - \cos(\theta_1 - \phi))]\right)^2 \\ &\quad + \left(\frac{r}{2}[\sin\theta_1 + \sin(\theta_1 - \phi) + t(\sin\theta_1 - \sin(\theta_1 - \phi))]\right)^2 \\ &= r^2\left[\cos^2(\phi/2) + t^2\sin^2(\phi/2)\right].\end{aligned}$$

Also, the distance ρ between two typical surface elements on the DNA and the CNT molecules is given by

$$\rho^2 = (a - \xi)^2 + z^2 + 4a\xi\sin^2(\theta_2/2),$$

where a is the radius of CNT, $r = 10$ Å, $c = 34$ Å, $-1 < t < 1$, $-\pi < \theta_2 < \pi$ and we have in mind the value $\phi = 12\pi/17$. Also, we have the interaction energy of point with infinite carbon nanotube from [4], which is given by

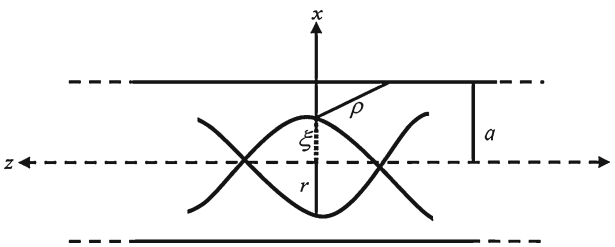

Fig. 2 Double-strand DNA molecule inside a single-walled carbon nanotube

Table 2 Approximate Lennard-Jones attractive and repulsive constants

	A (eV Å^6)	B (eV Å^{12})
C–C	56.21	191,800
C–H	10.52	20,700
C–N	60.09	177,400
C–O	63.08	160,600
C–P	115.6	539,300

$$E_c = \frac{3\pi^2\eta_g}{4a^4}\left[-AF\left(\frac{5}{2},\frac{5}{2};1;\left(\frac{\xi}{a}\right)^2\right)+\frac{21B}{32a^6}F\left(\frac{11}{2},\frac{11}{2};1;\left(\frac{\xi}{a}\right)^2\right)\right],$$

where η_g is the mean atomic surface density of CNT, and $F(a, b; c; z)$ is the standard hypergeometric function [10]. Thus, the total potential energy of the dsDNA with the CNT per unit length E, is given by

$$\begin{aligned} E &= \frac{rc\eta_{d_1}}{2\pi}\sin(\phi/2)\int_{-\pi}^{\pi}\int_{-1}^{1} E_c\left(1+\frac{4r^2\pi^2\sin^2(\phi/2)}{c^2}t^2\right)^{1/2} dt\, d\theta_2 \\ &= 2rc\eta_{d_1}\sin(\phi/2)\int_0^1 E_c\left(1+\frac{4r^2\pi^2\sin^2(\phi/2)}{c^2}t^2\right)^{1/2} dt, \end{aligned} \tag{1}$$

where η_{d_1} represents the mean atomic surface density of DNA for the helical phase angle $\phi = 12\pi/17$. The details for the analytical evaluation of (1) are presented in Appendix A from which we find that the total interaction energy for the DNA inside the CNT for any value of the helical phase angle ϕ is given by

$$E = \frac{3\pi^2 rc\eta_g\eta_{d_1}\sin(\phi/2)}{2a^4}\Big(-AR_3+\frac{21B}{32a^6}R_6\Big), \tag{2}$$

where R_n is defined by (4a).

3.1.1 Results and discussions for $\phi = 12\pi/17$

Although the final expression (2) with R_n defined by (4a) appear to be quite complicated, the numerical solution is readily obtained using the algebraic computer package MAPLE using the parameter values given in Table. 3. We show graphically in Fig. 3 the relation between the potential energy and the radius of the DNA (r) which are undertaken for each of the four specific armchair carbon nanotubes (i, i) for $i = 18, 19, 20$ and 21. As shown in Fig. 3, the radii of DNA molecules which minimize the interaction

Table 3 Numerical values of constants used in model

Radius of (18, 18) (Å)	12.21
Radius of (19, 19) (Å)	12.88
Radius of (20, 20) (Å)	13.56
Radius of (21, 21) (Å)	14.24
Mean surface density of carbon nanotube	$\eta_g = 0.3812$ Å^{-2}
Mean surface density of DNA ($\phi = 12\pi/17$)	$\eta_{d_1} = 0.97$ Å^{-2}
Mean surface density of DNA ($\phi = \pi$)	$\eta_{d_2} = 0.83$ Å^{-2}
Attractive constant CNT-DNA	$A = 42.563$ eV Å^6
Repulsive constant CNT-DNA	$B = 127,534.91$ eV Å^{12}

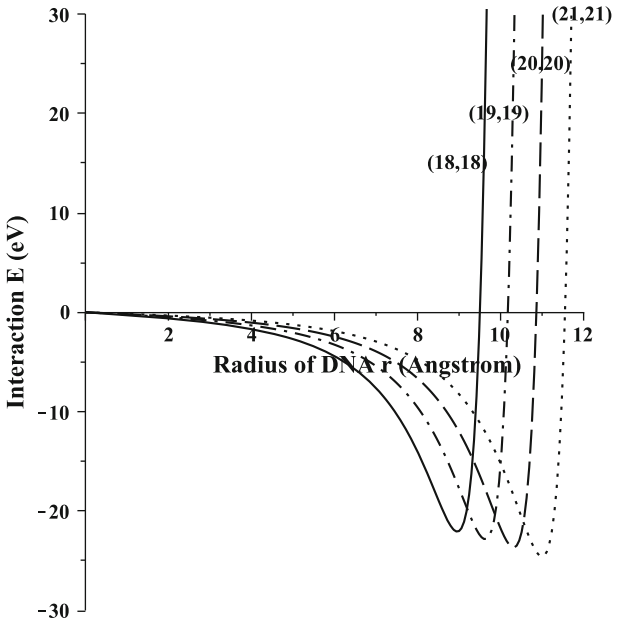

Fig. 3 Total interaction potential between DNA molecule inside (18, 18), (19, 19), (20, 20) and (21, 21) CNTs as function of DNA radius r for $\phi = 12\pi/17$

energy and which we refer to as the optimal radius are 8.96 Å, 9.63 Å, 10.31 Å and 11 Å for the (18, 18), (19, 19), (20, 20) and (21, 21) nanotubes, respectively. In addition, the larger the radius of the nanotube, the larger the optimal radius of DNA as larger radii nanotubes tend to accommodate larger DNAs. The DNA becomes unstable when the radii of DNA are beyond 9.48 Å, 10.17 Å, 10.85 Å and 11.54 Å for the (18, 18), (19, 19), (20, 20) and (21, 21) nanotubes, respectively due to the mutually repulsive force between the DNA and the nanotube. Also, Fig. 4 shows the interaction energy as a function of the radius of the CNT. We observe that the encapsulation of dsDNA inside carbon nanotubes may occur for radii greater than 12.28 Å. In addition, as shown in Fig. 4 if we vary the CNT radius the preferred radius of carbon nanotube giving the maximum energy to enclose the double helix DNA for this case ($\phi = 12\pi/17$) is about 12.71 Å, so we may infer that the (19, 19) tube is the preferred tube.

3.2 Special case $\phi = \pi$

In this section, we assume that the value of ϕ is equal to π. In this special case the formal analytical details are slightly simpler than those for the general case. Again the equilibrium position arises from the location of the minimum potential energy for the DNA molecule inside the CNT, and we begin by considering the interaction of a carbon nanotube with a single point located at a distance ξ from the tube axis, also as shown in Fig. 2. We then integrate the potential for a single point over the surface of the DNA molecule, and for the second integration we make the substitution $\xi = rt$.

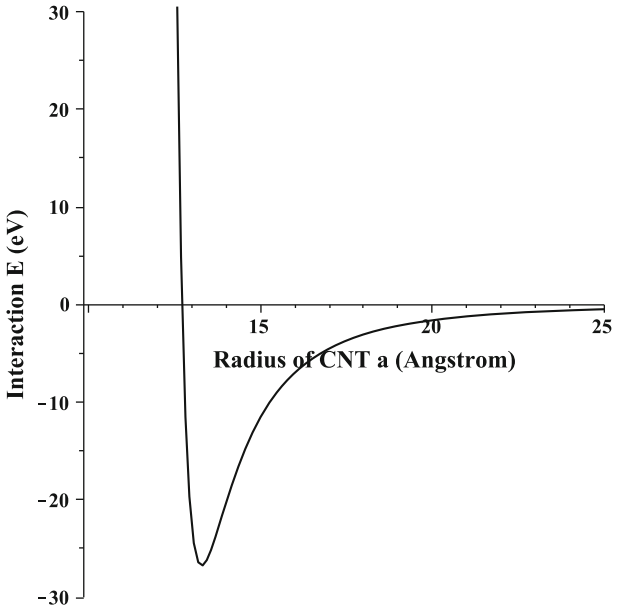

Fig. 4 Total interaction potential between DNA molecule and CNT as function of tube radius a for $\phi = 12\pi/17$

Also, the distance between two typical points ρ is given by

$$\rho^2 = a^2 + \xi^2 + z^2 - 2a\xi\cos\theta_2.$$

Now to evaluate the total interaction in this case we, follow the same steps as in the previous case, and we find that the total potential energy per unit length E for the offset DNA molecule in a carbon nanotube for $\phi = \pi$, is given by

$$E = \frac{3\pi^2 r c \eta_g \eta_{d_2}}{2a^4}\Big(- AI_3 + \frac{21B}{32a^6} I_6\Big), \tag{3}$$

where η_{d_2} represents the mean atomic surface density of DNA for the helical phase angle $\phi = \pi$. The formal details for the analytical evaluation of (3) are presented in Appendix B, and I_n is defined by (4b).

3.2.1 Results and discussions for $\phi = \pi$

The numerical solution is evaluated using the algebraic computer package MAPLE with the parameter values as given in Table 3. We show graphically in Fig. 5 the relation between the potential energy and the radius r of the DNA molecule. As shown in Fig. 5, the minimum energy is obtained when $r = 8.95$ Å, 9.61 Å, 10.30 Å and 10.99 Å for (18, 18), (19, 19), (20, 20) and (21, 21) carbon nanotubes, respectively. Thus, we observe that the optimal radii of the DNA which provide the lowest interaction energy

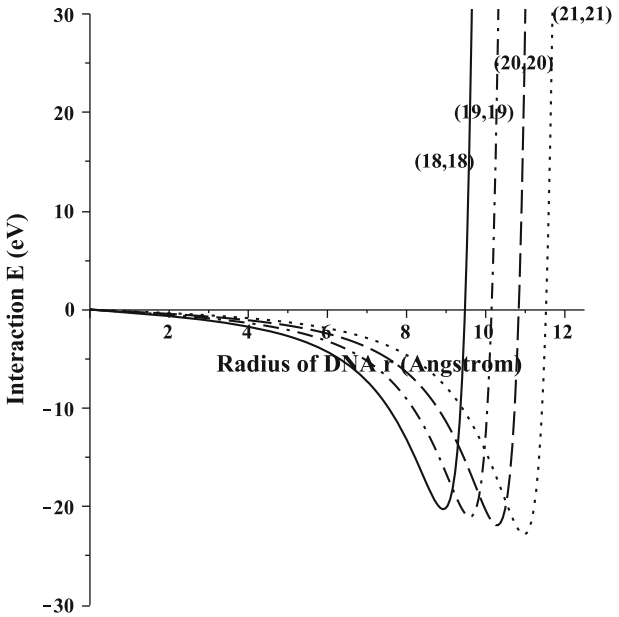

Fig. 5 Total interaction potential between DNA molecule inside (18, 18), (19, 19), (20, 20) and (21, 21) CNTs as function of DNA radius r for the special case $\phi = \pi$

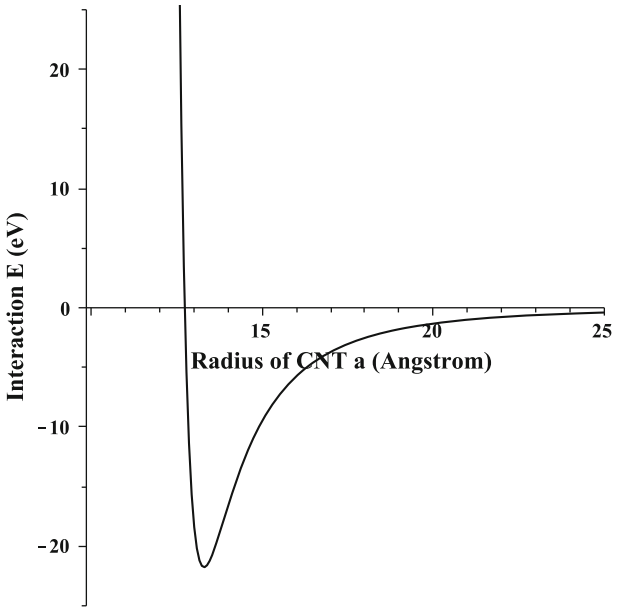

Fig. 6 Total interaction potential between DNA molecule and CNT as function of tube radius a for the special case $\phi = \pi$

for (18, 18), (19, 19), (20, 20) and (21, 21) carbon nanotubes are the radii of these tubes, respectively. In addition, these results give numerical values for the distances between the centre of the DNA and the wall of the nanotube. In addition, the larger the nanotube radius, the larger the optimal radius of DNA as a larger radius nanotube tends to accommodate larger DNAs. The DNA becomes unstable as the radius is increased beyond 9.47 Å, 10.17 Å, 10.84 Å and 11.52 Å for (18, 18), (19, 19), (20, 20) and (21, 21) carbon nanotubes, respectively due to the mutually repulsive force between the DNA and the nanotube. Also, as shown in Fig. 6 the preferred radius of carbon nanotube to enclose the double helix DNA in the special case $\phi = \pi$ is about 12.73 Å, so we infer that the (19, 19) tube is the preferred tube.

4 Summary

This paper presents a new applied mathematical model to investigate the interaction energy between a double-stranded DNA molecule (dsDNA) that is assumed to be inside a single-walled carbon nanotube. We employ the 6–12 Lennard–Jones potential together with the continuous approximation to calculate the van der Waals interaction energy which may be expressed in terms of the hypergeometric function. We examine the interaction energy for a dsDNA inside single-walled carbon nanotube for different armchair tubes, assuming that the DNA is already accepted into the tube. We refer to the location where the potential energy adopts the minimum value as the preferred optimal location. The numerical evaluations are performed using the algebraic computer package MAPLE. For the helical phase angle of the DNA, we study two cases for the interaction of the dsDNA inside a single-walled carbon nanotube, which are the general case with $\phi = 12\pi/17$, and a special case with $\phi = \pi$. In both cases we observe that at the point where the minimum energy occurs, that the difference between the radii of the CNT and the DNA is approximately 3.25 Å($a - r \approx$ 3.25 Å). In addition, the results indicate that the encapsulation of the dsDNA molecule into a single-walled carbon nanotubes may occur for carbon nanotubes with radii greater than 12.30 Å. Moreover, the optimal radius of carbon nanotube to enclose the double helix DNA in both cases is approximately 12.8 Å, and we conclude that the preferred tube is (19, 19). These results are close to those determined by Xue and Chen [26], who propose that the dsDNA molecule can be encapsulated inside a (20, 20) CNT. We comment that the mathematical modelling employed in deriving these results is computationally instantaneous, moreover, it compares favourably with other methods such as molecular dynamics simulations and experiments for example [17,26] which together may serve as a solid background for understanding DNA mechanics in carbon nanotubes.

Acknowledgments The first author would like to thank King Saud University (Saudi Arabia) for through the awarding of a PhD Scholarship.

Appendix A: Analytical evaluation of (1)

In this Appendix, we present the analytical details for the evaluation of (1). By defining the integral R_n as

$$R_n = \int_0^1 \left(1 + \frac{4r^2\pi^2 \sin^2(\phi/2)}{c^2} t^2\right)^{1/2} F\left(\frac{2n-1}{2}, \frac{2n-1}{2}; 1; \left(\frac{\xi}{a}\right)^2\right) dt,$$

since

$$\begin{aligned}\xi^2 &= r^2\left[\cos^2(\phi/2) + t^2 \sin^2(\phi/2)\right] \\ &= [r\cos(\phi/2))^2\left[1 + t^2 \tan^2(\phi/2)\right],\end{aligned}$$

thus

$$\begin{aligned}R_n = &\int_0^1 \left(1 + \frac{4r^2\pi^2 \sin^2(\phi/2)}{c^2} t^2\right)^{1/2} \\ &\times F\left((2n-1)/2, (2n-1)/2; 1; [r\cos(\phi/2)/a]^2\left[1 + t^2\tan^2(\phi/2)\right]\right) dt,\end{aligned}$$

on making the substitution $x = t^2 \Rightarrow dt = (1/2)x^{-1/2}dx$, when $t = 0 \Rightarrow x = 0$, and when $t = 1 \Rightarrow x = 1$, and by letting $\alpha = [2r\pi \sin(\phi/2)/c]^2$. Thus, the integral R_n becomes

$$\begin{aligned}R_n = &\frac{1}{2}\int_0^1 x^{-1/2}(1 + \alpha x)^{1/2} \\ &\times F\left((2n-1)/2, (2n-1)/2; 1; [r\cos(\phi/2)/a]^2\left[1 + x\tan^2(\phi/2)\right]\right) dx,\end{aligned}$$

and on using the generalized hypergeometric series [7], we may deduce

$$\begin{aligned}R_n = &\frac{1}{2}\sum_{m=0}^{\infty}\left(\frac{((2n-1)/2)_m\, r^m \cos^m(\phi/2)}{m! a^m}\right)^2 \\ &\times \int_0^1 x^{-1/2}(1 + \alpha x)^{1/2}\left[1 + x\tan^2(\phi/2)\right]^m dx,\end{aligned}$$

and by taking

$$H_m = \int_0^1 x^{-1/2}(1 + \alpha x)^{1/2}(1 + \beta x)^m dx,$$

where $\alpha = [2r\pi \sin(\phi/2)/c]^2$ and $\beta = \tan^2(\phi/2)$, then

$$(1+\beta x)^m = \sum_{p=0}^{m} \binom{m}{p} \beta^p x^p,$$

where $\binom{i}{j}$ is the binomial coefficient. Thus the integral H_m becomes

$$H_m = \sum_{p=0}^{m} \binom{m}{p} \beta^p \int_0^1 x^{p-1/2} (1+\alpha x)^{1/2}\, dx,$$

by using form in [7] (p. 59, Eq. (10)), thus

$$H_m = 2 \sum_{p=0}^{m} \binom{m}{p} \left[\beta^{2p}/(2p+1)\right] F(-1/2,\, p+1/2;\, p+3/2;\, -\alpha).$$

and we may deduce that R_n is given by

$$R_n = \frac{1}{2} \sum_{m=0}^{\infty} \sum_{p=0}^{m} \binom{m}{p} \left[\beta^{2p}/(2p+1)\right] \left(\frac{((2n-1)/2)_m\, r^m \cos^m(\phi/2)}{m! a^m} \right)^2 \times F(-1/2,\, p+1/2;\, p+3/2;\, -\alpha), \tag{4a}$$

and this expression completes (2).

Appendix B: Analytical evaluation of (3)

In this appendix we evaluate (3), By defining the integral I_n as

$$I_n = \int_0^1 \left(1 + \frac{4r^2\pi^2}{c^2} t^2\right)^{1/2} F\left(\frac{2n-1}{2}, \frac{2n-1}{2}; 1; \left(\frac{\xi}{a}\right)^2\right) dt,$$

since $\xi = rt$, thus

$$I_n = \int_0^1 \left(1 + \frac{4r^2\pi^2}{c^2} t^2\right)^{1/2} F\left((2n-1)/2, (2n-1)/2; 1; (rt/a)^2\right) dt,$$

on making the substitution $y = t^2 \Rightarrow dt = (1/2)y^{-1/2}dy$, when $t = 0 \Rightarrow y = 0$, and when $t = 1 \Rightarrow y = 1$, and by letting $\alpha^* = (2r\pi/c)^2$. Thus, the integral I_n becomes

$$I_n = \frac{1}{2}\int_0^1 y^{-1/2}\left(1+\alpha^* y\right)^{1/2} F\left((2n-1)/2, (2n-1)/2; 1; (r/a)^2\, y\right) dy,$$

using the generalized hypergeometric series [7], we may deduce

$$I_n = \frac{1}{2}\sum_{k=0}^{\infty}\left(\frac{((2n-1)/2)_k\, r^k}{k!a^k}\right)^2 \int_0^1 y^{k-1/2}\left(1+\alpha^* y\right)^{1/2} dy,$$

by using form in [7] (p. 59, Eq. (10)), thus

$$I_n = \sum_{k=0}^{\infty}\left(\frac{((2n-1)/2)_k\, r^k}{(2k+1)^{1/2}k!a^k}\right)^2 F\left(-1/2, k+1/2; k+3/2; -\alpha^*\right), \qquad (4b)$$

and this expression completes (3).

References

1. K.M. Abu-Salah, A.A. Ansari, S.A. Alrokayan, J. Biomed. Biotechnol. **15** (2010)
2. B. Alberts, A. Johnson, J. Lewis, M. Raff, K. Roberts, P. Walter, *Molecular Biology of the Cell*, 4th edn. (Garland Science, New York, 2002)
3. J.M. Bonard, N. Weiss, H. Kind, T. Stckli, L. Forr, K. Kern, A. Chtelain, Adv. Mater. **13**, 184–188 (2001)
4. B.J. Cox, N. Thamwattana, J.M. Hill, J. Phys. A Math. Theor. **41**, 27 (2008)
5. D. Cui, C.S. Ozkan, S. Ravindran, H.G.Y. Kong, Mech. Chem. Biol. **1**, 113–122 (2004)
6. E.K. Drexler, *Nanosystems: Molecular Machinery, Manufacturing, and Computation* (Wiley, Chichester, 1992)
7. A. Erdelyi, W. Magnus, F. Oberhettinger, F.G. Tricomi, *Higher Transcendental Functions, vol. I* (McGraw-Hill, USA, 1953)
8. H. Gao, Y. Kong, Annu. Rev. Mater. Res. **34**, 123–150 (2004)
9. L.A. Girifalco, M. Hodak, R.S. Lee, Phys. Rev. B **62**, 104–110 (2000)
10. I.S. Gradshteyn, I.M. Ryzhik, *Table of Integrals, Series, and Products*, 7th edn. (Academic Press, New York, 2007)
11. H. Hart, L.E. Craine, D.J. Hart, C.M. Hadad, *Organic Chemistry, A Short Course*, 12th edn. (Houghton Mifflin Company, Boston, 2007)
12. T.A. Hilder, J.M. Hill, Small **5**, 300–308 (2009)
13. J.O. Hirschfelder, C.F. Curtiss, R.B. Bird, *Molecular Theory of Gases and Liquids* (Wiley, New York, 1954)
14. T. Ito, L. Sun, R.M. Crooks, Chem. Commun. **13**, 1482–1483 (2003)
15. N.W.S. Kam, M. O'Connell, J.A. Wisdom, H. Dai, Proc. Natl. Acad. Sci. USA. **102**, 11600–11605 (2005)
16. S. Kilina, D.A. Yarotski, A.A. Talin, S. Tretiak, A.J. Taylor A.V. Balatsky, J. Drug. Deliv. **9** (2011), Proc. Natl. Acad. Sci. USA
17. E.Y. Lau, F.C. Lightstone, M.E. Colvin, Chem. Phys. Lett. **412**, 82–87 (2005)
18. H. Lodish, A. Berk, S.L. Zipursky, P. Matsudaira, D. Baltimore, J. Darnell, *Molecular Cell Biology*, 4th edn. (W.H.Freeman and Co Ltd, New York, 2000)

19. G. Lu, P. Maragakis, E. Kaxiras, Nano Lett. **5**, 897–900 (2005)
20. S.L. Mayo, B.D. Olafson, W.A. Goddard, J. Phys. Chem. **94**, 8897–8909 (1990)
21. T.W. Odom, J.L. Huang, P. Kim, C.M. Lieber, J. Phys. Chem. B **104**, 2794–2809 (2000)
22. M. Shim, K.N.W. Shi, R.J. Chen, Y. Li, H. Dai, Nano Lett. **2**, 285–288 (2002)
23. J.C. Wang, Proc. Natl. Acad. Sci. USA **76**, 200–203 (1979)
24. J.D. Watson, F.H. Crick, Nature **171**, 737–738 (1953)
25. Y. Xu, X. Mi, N.R. Aluru, Appl. Phys. Lett. **95**, 113–116 (2009)
26. Y. Xue, M. Chen, Nanotechnology **17**, 5216–5223 (2006)
27. M. Zheng et al., Science **302**, 1545–1548 (2003)
28. M. Zheng, A. Jagota, E.D. Semke, B.A. Diner, R.S. Mclean, S.R. Lustig, R.E. Richardson, N.G. Tassi, Nat. Mater. **2**, 338–342 (2003)